Stoichiometric δ-NbN: The Most Incompressible Cubic Transition Metal Mononitride

Jiao Tan, Shihao Zhang, Shanmin Wang, Wendan Wang, Xu Zheng, Jianfa Zhao, Wenmin Li, Xiaochun Mao, Ke Liu, Xiaolin Zhou,* Yusheng Zhao, Changqing Jin, and Xiaohui Yu**

We report the high-pressure synthesis and elastic properties of stoichiometric cubic δ-NbN investigated by a combination of experiments and first principles calculations. Using the high pressure solid-state ion-exchange reaction route, we have successfully synthesized polycrystalline δ-NbN at 5.5 GPa and 1673 K. The refined lattice parameter of as-synthesized sample is 4.3960(6) Å, corresponding to the stoichiometric niobium nitride. The determined bulk modulus of δ-NbN is $B_0 = 319(2)$ GPa with $B'_0 = 4.4(2)$, which is one of the most incompressible cubic transition metal mononitrides. Theoretical calculations of the elastic constants, bulk modulus, shear modulus, Young's modulus, and Poisson's ratio agree well with experimental and previous theoretical results. The calculated minimum shear strength of δ-NbN is 23.4 GPa for the (111)[$\bar{1}\bar{1}2$] slip system, comparable to those of ZrN and HfN. In addition, a finite density of states at the Fermi level was revealed for δ-NbN, hence exhibiting metallic behavior.

1. Introduction

Transition metal nitrides (TMN_x) are well-known for their perfect combination of various superior properties such as high hardness and melting points, low compressibility and electrical resistivity, and excellent chemical and thermal stability.[1–8] As a result, they have been widely used for cutting tools, abrasion-resistant coatings, turbine blades, etc.[1–3] In the large family of TMN_x, the face-centered-cubic structure niobium mononitride (δ-NbN) attracts particular interest for the additive high superconducting transition temperature ($T_C \sim 17.3$ K)[9] to the general characters. Theoretical and experimental studies have been extensively carried out to investigate various physical properties of δ-NbN involving hardness, structure stability, elasticity and its pressure dependence, superconductivity and its pressure dependence, Debye temperature, the relation of thermal expansion coefficient to temperature under pressure, etc.[5,9–17] Even other polymorphs of NbN have also been widely studied,[12,13,15] for example, hexagonal ε-NbN was recently reported to be a possible hard superconducting material with ultra-incompressibility and high shear rigidity by Zou et al.[18] However, there are still some issues for δ-NbN to be tackled: the difficulty in synthesizing stoichiometric δ-NbN, the accurate measurement for equation of state, the stress-strain relation upon shear, etc.

As is known, the stoichiometry is a key factor for the investigation (superconductivity, density, and elastic modulus, etc.) of TMN_x, because the nitrogen vacancy can substantially affect microstructure, bonding, and charge carrier density.[19–22] Particularly, it is reported that the bulk moduli decrease along with nitrogen deficiency for TiN, ZrN, and HfN.[21,22] Nevertheless, on account of the thermodynamically unfavorable formation of TMN_x, the synthesis of stoichiometric δ-NbN is usually difficult at ambient pressure.[23] Most of the synthesized samples from nitridation and ammoniation methods, pulsed laser deposition, and magnetron sputtering are usually either nonstoichiometric polycrystals or poorly-crystallized characterize-restricted thin films.[24–27] Considering the complex phase diagram, (e.g., hexagonal β-Nb_2N, ε-NbN, δ'-NbN, cubic δ-NbN, tetragonal γ-Nb_4N_3,) [24] it is even more difficult to prepare phase-pure stoichiometric δ-NbN with traditional methods. As a result,

J. Tan, X. Mao, Dr. K. Liu, Prof. X. Zhou
College of Physics and Electronic Engineering, Sichuan Normal University, Chengdu 610101, P. R. China
E-mail: lkworld@uestc.edu.cn; zhouxl_wuli@163.com

J. Tan, Dr. X. Zheng, Dr. J. Zhao, Dr. W. Li, Prof. C. Jin, Dr. X. Yu
Institute of Physics, Chinese Academy of Sciences, Beijing 100190, P. R. China
yuxh@iphy.ac.cn

Dr. S. Zhang
School of Materials Science and Engineering, Beihang University, Beijing 100191, P. R. China

Dr. S. Wang, Prof. Y. Zhao
Department of Physics, Southern University of Science & Technology, Shenzhen 518055, P. R. China

Dr. W. Wang
Sichuan Provincial Key Laboratory (for Universities) of High Pressure Science and Technology, Southwest Jiaotong University, Chengdu 610031, P. R. China

The ORCID identification number(s) for the author(s) of this article can be found under https://doi.org/10.1002/pssb.201700063.

Jiao Tan and Shihao Zhang contributed equally to this work.

DOI: 10.1002/pssb.201700063

most of previous experimental results are based on the non-stoichiometric δ-NbN_x samples with huge amount of nitrogen vacancies.

At present, there is, strictly speaking, a lack of reliable experimental study about the equation of state for δ-NbN. The derived bulk modulus (B_0), which pertinently reflecting the compressive resistant capacity, is important because it plays an irreplaceable role in the fundamental parameters and index of mechanical properties and technological applications. Up to now, there has been only one high pressure X-ray diffraction (XRD) experiment for δ-NbN by Chen et al. in 2005, which derived a B_0 value of 348 GPa with nonstoichiometric $NbN_{0.90(1)}$ samples [5,17]. Besides, the pressure transmission medium LiF adopted in the high pressure experiment could not provide hydrostatic pressure condition [5]. Thus, both of the non-stoichiometric and non-hydrostatic pressure conditions hinder an accurate compression experiments, leaving unauthentic bulk modulus of δ-NbN.

Recent years, a more effective method, high pressure solid-state ion-exchange reaction,[28] has been well developed to synthesize TMN_x. Generally, the reactants, ternary metal oxides and hexagonal boron nitride undergo an ion-exchange process (between metal and boron ion) and finally form TMN_x with easily-remove byproducts.[29] Using this method, well-crystallized stoichiometric mononitrides such as CrN,[23] VN,[30] MoN,[31] WN, and even novel materials as hexagonal and rhombohedral W_2N_3[28] have been successfully synthesized, which tremendously accelerates the fundamental researches of TMN_x. In this work, we extended this method to synthesize stoichiometric δ-NbN, with which we investigated its equation of state by high pressure synchrotron XRD experiments. In addition, first principles calculations with generalized-gradient approximation were complemented to study its elastic and plastic mechanical properties.

2. Experimental and Theoretical Details

High-purity potassium niobium oxide ($KNbO_3$) (99.999%) and hexagonal boron nitride (*h*BN) (99.9%) powders were mixed homogeneously in a molar ratio of 3:5 as starting materials. Then the powder mixture was compressed into a cylindrical molybdenum capsule with inner diameter and height of 6 and 2 mm, respectively mainly to eliminate the amount of uncertainty of *h*BN, because in the high-pressure cell assembly, out of the molybdenum capsule were *h*BN capsule, graphite furnace and pyrophyllite in turn. Putting the assembly into a cubic press, the reactants gained a reaction condition of 5.5 GPa and 1673 K. After heated for 90 min until quenching to room temperature, the sample was decompressed to atmosphere pressure. The as-prepared sample was ground first with an agate mortar to identify the ingredients, and then dealt with nitric acid (HNO_3) to remove the byproducts. The identification of both as-prepared and as-purified sample was carried out on an X-ray diffractometer with a copper target ($\lambda_{Ka1} = 1.5406$ Å). The Rietveld refinement of the obtained XRD data was performed with GSAS software.[32] To obtain equation of state and bulk modulus, high pressure angle-dispersive synchrotron XRD experiment with a diamond anvil cell (DAC) was carried out at the 16BM-D beamline of the Advanced Photon Source High Pressure Collaborative Access Team (Argonne National Laboratory, Argonne, IL). With ruby serving as the pressure calibration material, the experiment achieved pressure of 31.7 GPa. δ-NbN sample in stoichiometric composition and gaseous neon medium, providing isostatic pressure, were used to ensure the accuracy of B_0 value.

First principles calculations were carried out using the VASP code[33] with the Perdew-Burke-Ernzerhof (PBE) version[34] of the Generalized Gradient Approximation (GGA) as the exchange-correlation functional. Specifically, single-crystal elastic constants were calculated using efficient strain-energy method. The bulk modulus, shear modulus, Young's modulus, and Poison ratio were derived from our calculated elastic constants by means of Voigt-Reuss-Hill approximation. The stress-strain relations upon shear for δ-NbN were calculated in four main crystallographic directions through projection of a unit cell onto the corresponding crystal axes with one axis parallel to the slip direction and another axis perpendicular to the slip plane. The calculation details can be referred to the previous works.[8,35–37]

3. Results and Discussion

Figure 1 shows the X-ray diffraction pattern collected with a copper target ($\lambda_{Ka1} = 1.5406$ Å) at room temperature and ambient pressure for the as-purified sample from the high pressure synthesis. Based on the identification of all Bragg diffraction peaks, the sample was determined as face-centered-cubic structure δ-NbN with space group of $Fm\bar{3}m$ (No. 225). The formation process of NbN from $KNbO_3$ and *h*BN can be referred to the similar preparation of VN from $NaVO_3$ and *h*BN.[30] With Rietveld method, the lattice parameter was refined as $a = 4.3960(6)$ Å, slightly larger than the reported

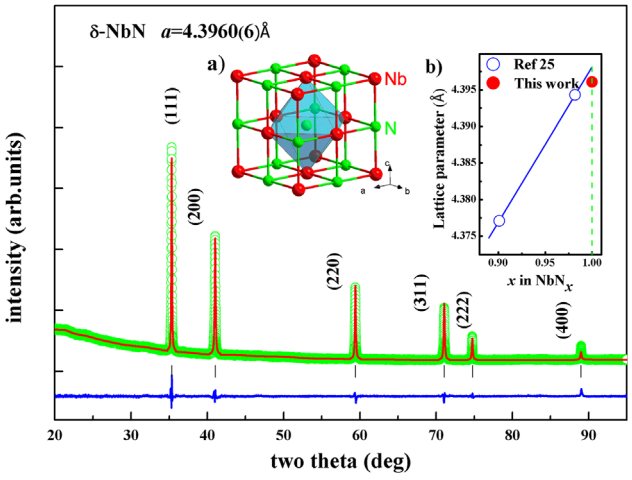

Figure 1. Refined XRD pattern collected with a copper target ($\lambda_{Ka1} = 1.5406$ Å) for as-purified δ-NbN. Green circles and red lines represent the observed and calculated profiles, respectively. Blue lines in the bottom correspond to the difference between the observed and calculated profiles. Black tick marks denote the peak positions. The inset a) presents the crystal structure of δ-NbN, while the inset b) shows the partial *a*–*x* relationship of δ-NbN_x according to Ref. [25].

value 4.394(3) Å for $NbN_{0.98(2)}$.[38] According to the *a-x* (lattice parameter-*x* in NbN) relationship plotted by Brauer et al., the lattice parameter increases linearly with nitrogen content when approaches the stoichiometric molar ratio for δ-NbN.[39] With a larger lattice parameter, our synthesized samples should be closer to stoichiometry than $NbN_{0.98(2)}$. According to the results of Christensen et al.,[25] a partial *a-x* relationship was plotted, showing that our sample was stoichiometric within reasonable error. On the other hand, the optimized lattice parameter of stoichiometric δ-NbN from first principles calculations was 4.419 Å, which was in agreement with our measured data within reasonable error bars from theoretical approximation as other calculated values ($a = 4.41$Å,[11] $a = 4.42$Å[10]). Apparently, such a high pressure method is proved to be effective for preparing stoichiometric δ-NbN. The superiority of high pressure condition for yielding stoichiometric compounds without nitrogen deficiency and even high nitrogen concentration nitrides might originate from its effective function for depressing nitrogen decomposition and promoting the bonding of d-electrons.[30,40]

With the synthesized stoichiometric samples, we further studied the high pressure equation of state of δ-NbN in a DAC. As is shown in **Figure 2**, all diffraction peaks from the angle-dispersive synchrotron XRD experiment remained invariant except for a consistent right shift, meaning that δ-NbN was structurally stable without phase transition at high pressure up to 31.7 GPa. **Figure 3** presents the pressure-relative volume curves from the compression test. The third order Birch-Murnaghan EOS (equation of state),[41]

$$P = \frac{3}{2}B_0\left[\left(\frac{V}{V_0}\right)^{-7/3} - \left(\frac{V}{V_0}\right)^{-5/3}\right]\left\{1 - \frac{3}{4}(4 - B'_0)\left[\left(\frac{V}{V_0}\right)^{-2/3} - 1\right]\right\}, \quad (1)$$

was used to fit the experimental data, yielding the bulk modulus $B_0 = 319(2)$ GPa and its first pressure derivative $B'_0 = 4.4(2)$. Fixing B'_0 at the conventional value 4, we obtained

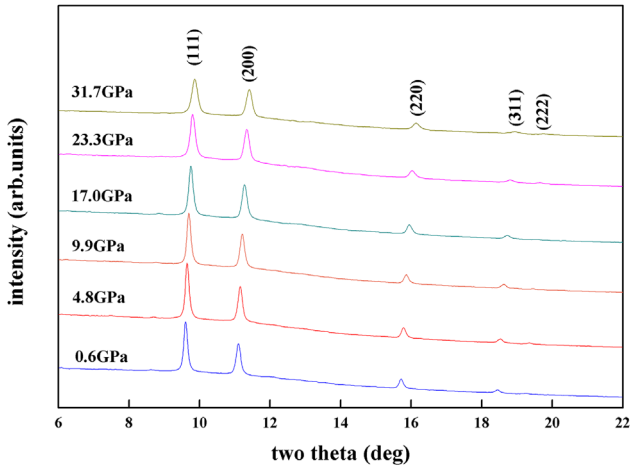

Figure 2. Partial high pressure angle-dispersive synchrotron XRD patterns of δ-NbN at pressures varying from 0.6 to 31.7 GPa. Ruby was used to calibrate the pressure in the diamond anvil cell. Gaseous neon was chosen as pressure medium.

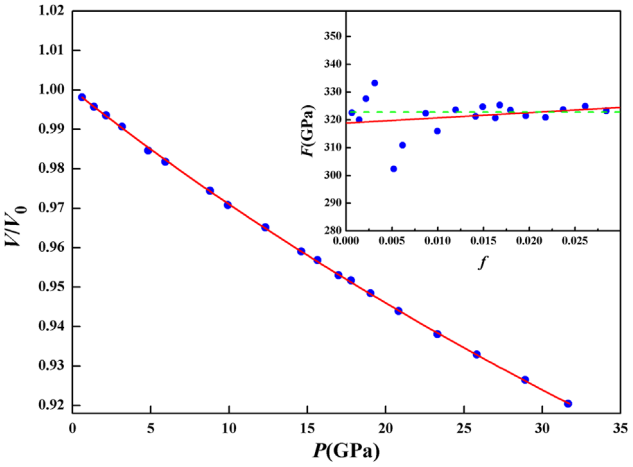

Figure 3. Pressure-relative volume relation of δ-NbN. The zero-pressure unit-cell volume was 84.95(5) Å^3 derived from the ambient pressure XRD. The red solid line denotes the third order Birch-Murnaghan fit to the measured data. The inset shows the normalized pressure (*F*)–Eulerian strain (*f*) relation for the compression test. The red solid line represents the third order Birch-Murnaghan fit, while the green dashed line denotes the second Birch-Murnaghan fit.

$B_0 = 323(1)$ GPa from the second order Birch-Murnaghan EOS. To better examine the experimental uncertainties, the *F–f* relation was also plotted in the inset, where the normalized pressure (*F*) and Eulerian strain (*f*) were written as $F = P/\left[3f(1+2f)^{5/2}\right]$ and $f = \left[(V/V_0)^{-2/3} - 1\right]/2$, respectively. For the linear *F-f* relation, the bulk modulus B_0 just can be represented by the intercept, and B'_0 can be also derived from the slope. Here the horizontal and slant lines denote the second and third order Birch-Murnaghan fits, respectively. Observing the experimental data points and the fit lines, it can be confirmed that our fit results are reasonable within the experimental uncertainties. In consideration of the potential influence on B_0 value from the alternative equation of states, we simultaneously fitted the data to the Vinet EOS,[42]

$$P = \frac{3B_0(1-x)}{x^2}\exp\left[\frac{3}{2}(B'_0 - 1)(1-x)\right], \quad (2)$$

with $x = (V/V_0)^{1/3}$, leading to $B_0 = 318(2)$ GPa with $B'_0 = 4.5(2)$ or $B_0 = 323(1)$ GPa for $B'_0 = 4$. Evidently, the choice of EOS has little influence on the B_0 value of δ-NbN, and the result from the commonly used Birch-Murnaghan EOS could be reasonably employed as the finally accurate result.

With $B_0 = 319(2)$ GPa, more incompressible than most of the face-centered-cubic structure transition metal mononitrides [such as δ-ZrN ($B_0 = 248$ GPa), δ-HfN ($B_0 = 260$ GPa) [5], c-CrN ($B_0 = 257$ GPa)[43], and even γ-MoN ($B_0 = 307$ GPa)[31] etc.] as shown in **Table 1**, δ-NbN is proved to be the most incompressible cubic transition metal mononitride, and successfully edges itself into those possessing high bulk modulus ($B_0 > 300$ GPa).[48] At present, the fundamental of bulk modulus is still incompletely clear to us, but a large valence electron density (electrons/unit volume) is believed to make for B_0

Table 1. Experimental results of B_0 and B'_0 for partial transition metal mononitrides with face-centered-cubic structure.

	a^0 (Å)	B_0 (GPa)	B'_0	Method	Pressure medium	Ref.
TiN	4.24	289(7)	2.5(8)	HP-SXRD[a]	N_2	[44]
δ-ZrN		248	4 fixed	HP-SXRD[a]	silicon oil	[5]
δ-HfN		260	4 fixed	HP-SXRD[a]	silicon oil	[5]
δ-VN	4.1349(9)	300(6)	3.6(6)	HP-SXRD[a]	argon	
		296(2)	4 fixed			[45]
δ-NbN	4.3960(6)	319(2)	4.4(2)	HP-SXRD[a]	neon	This work
		323(1)	4 fixed			
	4.379(2)	348	4 fixed	HP-SXRD[a]	LiF	[5]
		292		Neutron[b]		[5]
		287		acoustic method[c]		[45,46]
δ-TaN	4.3409(1)	295(1)	4 fixed	HP-SXRD[a]	methanol-ethanol -water(16:3:1)	[47]
c-CrN	4.1513(2)	257	4 fixed	HP-SXRD[a]	neon	[43]
γ-MoN	4.1925(3)	307	4 fixed	HP-SXRD[a]	helium	[31]

[a] High pressure synchrotron X-ray diffraction experiments.
[b] Derive B_0 value from the initial slopes of phonon dispersion curves measured by coherent inelastic neutron scattering.[5]
[c] Yield elastic constants from the measured surface acoustic dispersion curves.[45]

enlargement.[48,49] With valence electron density of 0.705 and 0.5102 electrons Å^{-3}, diamond and OsB_2 show bulk modulus of 442 and 395 GPa, respectively.[49] It is no surprise that δ-NbN possesses a large B_0 because its valence electron density is large as 0.4708 electrons Å^{-3}. In addition, the large bulk modulus for δ-NbN might be also correlated with the high cohesive energy of niobium with half-filled shells.[49] As to what truly determines the bulk modulus, it remains to be confirmed. Nevertheless, such a large B_0 value for δ-NbN might be helpful to further understand the origin of incompressibility.

Compared with the $B_0 = 348$ GPa of Chen et al.,[5] our result is smaller. This might be caused by different pressure transmission mediums used in compression experiments. In the nonhydrostatic pressure condition, the pressure in the direction approximatively perpendicular to the DAC axis will be considerably smaller than that along the DAC axis. Therefore the actually measured variation of unit-cell volume or lattice constant, which is only associated with the compression in the direction approximately perpendicular to the DAC axis, will weaken (i.e., the measured B_0 will be larger). On the other hand, it cannot be concluded regarding how nitrogen vacancies affect the bulk modulus of δ-NbN because two different factors (nitrogen concentrations and pressure mediums) exist between the two experiments. Thus, a hydrostatic compression experiment for nonstoichiometric sample is still needed to confirm whether the bulk modulus of δ-NbN decreases with the nitrogen escape from stoichiometry composition as group 4 transition metal nitrides do. Except for the high pressure synchrotron experiment, the bulk modulus of δ-NbN has also been derived from phonon dispersion curves measured by neutron scattering ($B_0 = 292$ GPa)[5] and acoustic measurements ($B_0 = 287$ GPa),[45,46] but the results have a certain difference compared with ours. It is probably due to the sample imperfections (impurities, cracks, pores, etc.) for acoustic measurements and the effect of theoretical models for neutron scattering, while the high pressure synchrotron X-ray diffraction experiment is the most reliable method to measure bulk modulus for it is unacted on above sample imperfections and theoretical models.[45]

In order to figure out the physical mechanism underlining the high incompressibility, we perform the first principles calculations. As is shown in **Table 2**, three independent single-crystal elastic constants of δ-NbN obtained in the present study are $C_{11} = 706$ GPa, $C_{12} = 110$ GPa, and $C_{44} = 93$ GPa, in agreement with previous theoretical values, $C_{11} = 705$ GPa[13] (696.2 GPa,[14] 722 GPa[15]), $C_{12} = 115$ GPa[13] (112.6 GPa,[14] 108 GPa[15]), and $C_{44} = 82$ GPa[13] (85.9 GPa,[14] 88 GPa[15]). The reasons why the experimental values of C_{ij} from acoustic measurements and neutron scattering can't agree well with our results as well as other theoretical values might be the previously mentioned sample imperfections and theoretical models, respectively. From the calculated elastic constants, the derived bulk modulus is $B = 309$ GPa, which agrees with our experimental result, that is 319(2) GPa, from the equation of state, reflecting the reliability of our calculations. Different from the bulk modulus, it is relatively difficult to measure experimentally for the shear modulus, a fundamental quantity descripting the resistance to reversible deformations upon shear stress.[6] By means of Voigt-Reuss-Hill approximation, the theoretically obtained shear modulus is $G = 152$ GPa, which is a little small than δ-ZrN ($G = 176$ GPa) and δ-HfN ($G = 197$ GPa). The derived Young's modulus is $E = 392$ GPa, agreeing well with the previous results 368 GPa[13] and 385 GPa.[15] Another important parameter Poison ratio, reflecting the ratio of the contraction strain to the corresponding extension strain, is theoretically obtained as $\nu = 0.290$, which is reasonable agreement with previous theoretical values (i.e., 0.30,[13] 0.29[15]), close to the typical value $\nu = 0.33$ for metallic

Table 2. Experimental and theoretical results of elastic constants (C_{ij}), bulk modulus (B_0), shear modulus (G), Young's modulus (E) and Poisson's ratio (ν) of δ-NbN.

C_{11} (GPa)	C_{12} (GPa)	C_{44} (GPa)	B_0 (GPa)	G (GPa)	E (GPa)	ν	Method	Ref.
706	110	93	309	152	392	0.290	GGA[a]	This work
			319(2)				HP-SXRD	
739	161	76	354	161		0.18	LDA[b]	
608	134	117	292	165		0.18	Neutron	
			348				HP-SXRD	[5]
705	115	82	312	141	368	0.30	GGA[a]	[13]
696.2	112.6	85.9	307.2	144.0			GGA[a]	[14]
722	108	88	312	149	385	0.29	LDA[b]	[15]
630	134	85	299	133	346	0.307	GGA[a]	[16]
			317				GGA[a]	
			354				LDA[b]	[10]
692	113	84	306	187		0.14	GGA[a]	
806	119	89	348	216		0.13	LDA[b]	[11]
556	152	125	287				Acoustic method	[45,46]

[a] The first-principles calculations with generalized gradient approximation.
[b] The first-principles calculations with local density approximation.

materials.[49,50] For cubic crystals, the elastic anisotropy can be described with the anisotropy index A,[51] which is expressed as $A = 2\,C_{44}/(C_{11}-C_{12})$ and denotes isotropic while $A = 1$. The derived $A = 0.31$ demonstrates the elastic anisotropy of δ-NbN.

To better understand its mechanical property, the anisotropic shear strengths have been also studied theoretically by calculating the stress-strain relations upon shear for δ-NbN in four slip systems, that is (110)[1$\bar{1}$0], (111)[1$\bar{1}$0], (111)[11$\bar{2}$], and (111)[$\bar{1}\bar{1}$2]. Because what the Shear modulus describes is merely the resistance to elastic deformations at small shear strains, while the ideal shear strength describes the resistance to plastic deformations upon large strains. For a stress-strain curve, the maximum stress represents the ideal shear strength along a certain deformation path, after which the lattice/electronic instability occurs.[52] As is shown in **Figure 4**, the critical stresses of lattice/electronic instability in the four slip systems are different, illustrating the anisotropic resistance to plastic deformations for δ-NbN. The ideal shear strength for (111)[11$\bar{2}$] slip system is the largest among the four slip systems, while weakest deformation path is along (111)[$\bar{1}\bar{1}$2] slip system. The minimum ideal shear strength of δ-NbN is 23.4 GPa, comparable to those of ZrN (26.1 GPa) and HfN (26.7 GPa) for the same slip systems (111)[$\bar{1}\bar{1}$2].[53] Describing the resistance to plastic deformation, elastic deformation upon shear, reversible volume change, respectively, the three physical quantities, shear strength, shear modulus, and bulk modulus, are all very important for studying mechanical property. Therefore, the three physical quantities of δ-NbN are compared with other transition metal nitrides as well as *c*BN in **Table 3**. With high bulk modulus

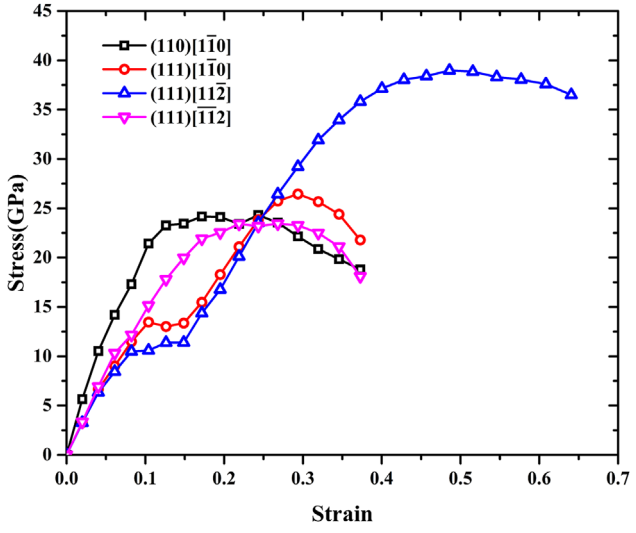

Figure 4. Stress-strain relationships under shear deformations calculated by *ab initio* DFT for δ-NbN.

Table 3. The minimum shear strength (τ_{min}) and corresponding slip system, shear modulus (G), and bulk modulus (B_0) of some transition metal nitrides and *c*BN.

	τ_{min} (GPa)	Slip system	G (GPa)	B_0 (GPa)	Ref.
NbN	23.4	(111)[$\bar{1}$ $\bar{1}$2]	152	319	This work
TiN	28.8	(111)[$\bar{1}$ $\bar{1}$2]	201	289	[44,53]
ZrN	25.9	(110)[1$\bar{1}$0]	176	248	[5,53]
HfN	26.5	(110)[1$\bar{1}$0]	197	260	[5,53]
Re_2N	12.4	(0001)[10$\bar{1}$0]	182	401	[7]
Re_3N	15.5	(0001)[10$\bar{1}$0]	203	397	[7]
cBN	58.3	(111)[11$\bar{2}$]	390	376	[36]

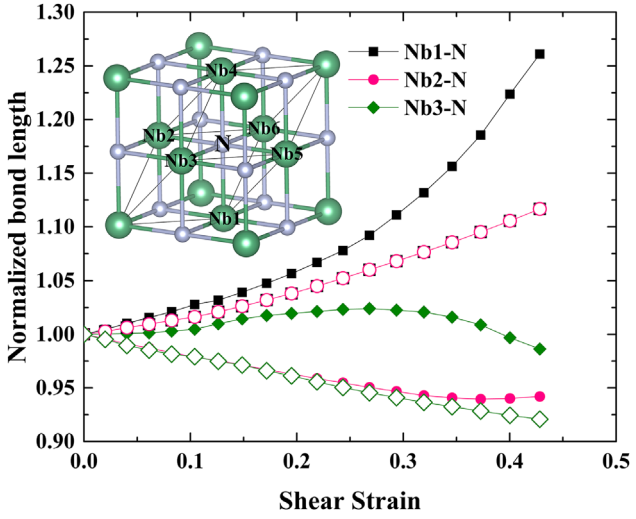

Figure 5. Variations of normalized bond lengths with (111)[1$\bar{1}$0] (solid) and (111)[11$\bar{2}$] (open) shear strain.

and relatively high shear strength, δ-NbN possesses comparatively satisfactory mechanical properties. Noting that there are nonmonotonic behaviors for the curves of (111)[1$\bar{1}$0] and (111)[11$\bar{2}$] (see Figure 4), variations of normalized bond lengths with (111)[1$\bar{1}$0] and (111)[11$\bar{2}$] shear strain have been further calculated as shown in **Figure 5**. By symmetry, the Nb4-N, Nb5-N, and Nb6-N bond lengths are equal to those of Nb1-N, Nb2-N, and Nb3-N, respectively. It is seen that there is not obvious inflection at the strain values where the inflection (minima) exists at the stress-strain curves. It is indicated that the inflection (minima) at the stress-strain curves is not due to the structural transformation. We have also calculated the partial

Table 4. The changes of the partial DOS at the Fermi level along (111)[1$\bar{1}$0] and (111)[11$\bar{2}$] slip systems.

Strain along (111)[1$\bar{1}$0]	Nb_p	Nb_d	N_p
0.0000	0.00169	0.60487	0.06899
0.1262	0.00359	0.64791	0.08351
0.2190	0.00628	0.58541	0.08081
Strain along (111)[11$\bar{2}$]	Nb_p	Nb_d	N_p
0.0000	0.00169	0.60487	0.06899
0.1487	0.00813	0.4777	0.09238
0.2190	0.00883	0.41435	0.07858

DOS at shear strain of (a) 0.0000, (b) 0.1262 (at minima), and (c) 0.2190 (after minima) along the (111)[1$\bar{1}$0] slip system, and (d) 0.0000, (e) 0.1487 (at minima), and (f) 0.2190 (after minima) along the (111)[11$\bar{2}$] slip system, and the results are shown as **Figure 6**. The changes of the partial DOS at the Fermi level are summarized as **Table 4**. It is found that there is a different trend, that is increase and then decrease, for the partial DOS of Nb_d and N_p along (111)[1$\bar{1}$0] and N_p for (111)[11$\bar{2}$], which indicates an electronic instable maybe happen at the minima, like the previous report of ReB_2.[54] The calculation of electronic structure may provide an alternate view of the nonmonotonic behaviors in the shear deformation of δ-NbN, which is however beyond the scope of the present paper. It does not influence the final result of ideal strength as the lowest shear strength is found along the (111)[$\bar{1}\bar{1}$2] shear deformation path. **Figure 7** illustrates the energy band structure and partial density of states (PDOS) of δ-NbN. It is seen that δ-NbN phases show finite DOS at the Fermi level and hence exhibit metallic behavior.

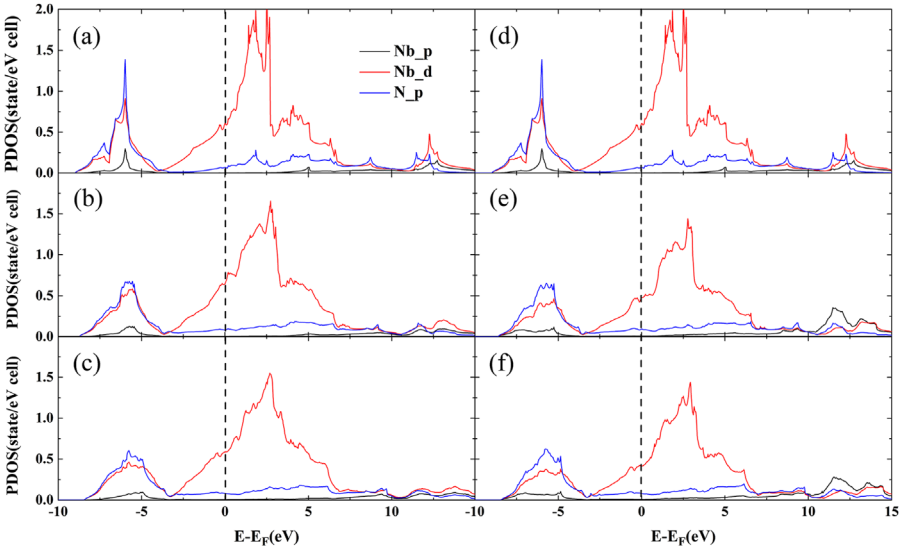

Figure 6. The partial DOS at shear strain of (a) 0.0000, (b) 0.1262 (at minima) and (c) 0.2190 (after minima) along the (111)[1$\bar{1}$0] slip system, and (d) 0.0000, (e) 0.1487 (at minima) and (f) 0.2190 (after minima) along the (111)[11$\bar{2}$] slip system.

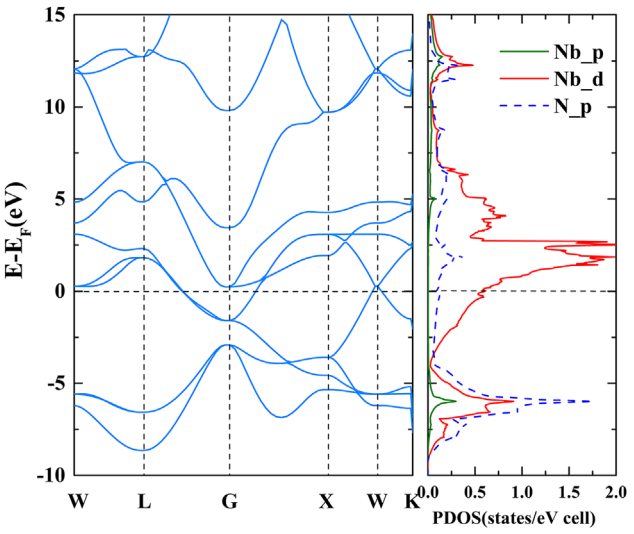

Figure 7. Energy band structure and partial density of states (PDOS) for δ-NbN. The red solid and blue dashed curves are from Nb d orbital and N p orbital. The vertical dashed line indicates the Fermi level.

4. Conclusions

In this work, we successfully synthesized stoichiometric δ-NbN with high pressure solid-state ion-exchange reaction route and accurately measured its bulk modulus through high pressure angle-dispersive synchrotron X-ray diffraction experiment with a diamond anvil cell. Simultaneously, complementary first principles calculations with generalized-gradient approximation were performed for δ-NbN. Through the isostatic compression test for the prepared stoichiometric sample with lattice parameter of 4.3960(6) Å, we derived bulk modulus $B_0 = 319(2)$ GPa with $B'_0 = 4.4(2)$ for δ-NbN, proved to be one of the most incompressible cubic transition metal mononitrides. The calculated lattice constant of 4.419 Å and bulk modulus of 309 GPa are in agreement with our experimental results within reasonable errors. Shear modulus $G = 152$ GPa, Young's modulus $E = 392$ GPa, and Poisson's ratio $\nu = 0.290$ were also theoretically obtained. The calculated minimum shear strength of δ-NbN is 23.4 GPa for the (111)$[\bar{1}\bar{1}2]$ slip system, comparable to those of ZrN and HfN. In addition, the metallic behavior of δ-NbN was suggested, as illustrated by the finite density of states at the Fermi level.

Acknowledgements

This work is supported by the National Key R&D Program of China (2016YFA0401530), the National Natural Science Foundation of China (Grant No. 11575288, 51402350, and 11027405), the Scientific Research Fund of Sichuan Provincial Education Department (Grant No. 15ZA0033), and the International Cooperation Projects Foundation of Sichuan Provincial Science and Technology Department (Grant No. 2014HH0014). S. Wang and Y. Zhao acknowledge the Shenzhen Peacock Plan (No. KQTD2016053019134356). The compressibility experiment is conducted at the 16BM-D beamline of Advanced Photon Source, Argonne National Lab.

Conflict of Interest

The authors declare no conflict of interest.

Keywords

bulk modulus, equation of state, high-pressure synthesis, niobium nitride

Received: February 9, 2017
Revised: August 3, 2017
Published online: August 24, 2017

[1] L. E. Toth, *Transition Metal Carbides and Nitrides*, Academic Press, New York, London **1971**.
[2] S.-H. Jhi, J. Ihm, S. G. Louie, M. L. Cohen, *Nature* **1999**, *399*, 132.
[3] A. Zerr, G. Miehe, R. Riedel, *Nat. Mater.* **2003**, *2*, 185.
[4] R. F. Zhang, D. Legut, Z. H. Fu, S. Veprek, Q. F. Zhang, H. K. Mao, *Phys. Rev. B* **2015**, *92*, 104107.
[5] X. J. Chen, V. V. Struzhkin, Z. Wu, M. Somayazulu, J. Qian, S. Kung, A. N. Christensen, Y. Zhao, R. E. Cohen, H.-K. Mao, R. J. Hemley, *Proc. Natl. Acad. Sci. USA* **2005**, *102*, 3198.
[6] A. F. Young, C. Sanloup, E. Gregoryanz, S. Scandolo, R. J. Hemley, H.-K. Mao, *Phys. Rev. Lett.* **2006**, *96*, 155501.
[7] R. F. Zhang, Z. J. Lin, H.-K. Mao, Y. Zhao, *Phys. Rev. B* **2011**, *83*, 060101.
[8] K. Liu, S. M. Wang, X. L. Zhou, J. Chang, *J. Appl. Phys.* **2013**, *114*, 063512.
[9] K. S. Keskar, T. Yamashita, Y. Onodera, *Jpn. J. Appl. Phys.* **1971**, *10*, 370.
[10] C. Stampfl, W. Mannstadt, R. Asahi, A. J. Freeman, *Phys. Rev. B* **2001**, *63*, 155106.
[11] W. Chen, J. Z. Jiang, *J. Alloys Compd.* **2010**, *499*, 243.
[12] A. T. A. Meenaatci, R. Rajeswarapalanichamy, K. Iyakutti, *Solid State Sci.* **2013**, *19*, 36.
[13] Z. H. Wang, X. Y. Kuang, X. F. Huang, P. Lu, A. J. Mao, *EPL* **2010**, *92*, 56002.
[14] D. H. Ren, X. L. Cheng, *Chin. Phys. B* **2012**, *21*, 127103.
[15] E. Zhao, J. Wang, J. Meng, Z. Wu, *Comput. Mater. Sci.* **2010**, *47*, 1064.
[16] B. D. Fulcher, X. Y. Cui, B. Delley, C. Stampfl, *Phys. Rev. B* **2012**, *85*, 184106.
[17] X. J. Chen, V. V. Struzhkin, Z. Wu, R. E. Cohen, S. Kung, H.-K. Mao, R. J. Hemley, *Phys. Rev. B* **2005**, *72*, 094514.
[18] Y. Zou, X. Wang, T. Chen, X. Li, X. Qi, D. Welch, P. Zhu, B. Liu, T. Cui, B. Li, *Sci. Rep.* **2015**, *5*, 10811.
[19] T. Lee, K. Ohmori, C.-S. Shin, D. G. Cahill, I. Petrov, J. E. Greene, *Phys. Rev. B* **2005**, *71*, 144106.
[20] H.-S. Seo, T.-Y. Lee, I. Petrov, J. E. Greene, D. Gall, *J. Appl. Phys.* **2005**, *97*, 083521.
[21] N. J. Ashley, R. W. Grimes, K. J. Mcclellan, *J. Mater Sci.* **2007**, *42*, 1884.
[22] N. J. Ashley, D. Parfitt, A. Chroneos, R. W. Grimes, *J. Appl. Phys.* **2009**, *106*, 083502.
[23] M. Chen, S. Wang, J. Zhang, D. He, Y. Zhao, *Chem. Eur. J.* **2012**, *18*, 15459.
[24] G. Brauer, *J. Less Common Met.* **1960**, *2*, 131.
[25] A. N. Christensen, S. Fregerslev, *Acta Chem. Scand. A* **1977**, *31*, 861.
[26] R. E. Treece, J. S. Horwitz, J. H. Claassen, D. B. Chrisey, *Appl. Phys. Lett.* **1994**, *65*, 2860.
[27] R. Baskaran, A. V. T. Arasu, E. P. Amaladass, M. P. Janawadkar, *J. Appl. Phys.* **2014**, *116*, 163908.
[28] S. Wang, X. Yu, Z. Lin, R. Zhang, D. He, J. Qin, J. Zhu, J. Han, L. Wang, H.-K. Mao, J. Zhang, Y. Zhao, *Chem. Mater.* **2012**, *24*, 3023.
[29] L. Lei, W. Yin, X. Jiang, S. Lin, D. He, *Inorg. Chem.* **2013**, *52*, 13356.

[30] S. Wang, X. Yu, J. Zhang, L. Wang, K. Leinenweber, D. He, Y. Zhao, *Cryst. Growth Des.* **2016**, *16*, 351.
[31] S. Wang, D. Antonio, X. Yu, J. Zhang, A. L. Cornelius, D. He, Y. Zhao, *Sci. Rep.* **2015**, *5*, 13733.
[32] B. H. Toby, *J. Appl. Crystallogr.* **2001**, *34*, 210.
[33] G. Kresse, J. Furthmüller, *Comput. Mater. Sci.* **1996**, *6*, 15.
[34] J. P. Perdew, K. Burke, M. Ernzerhof, *Phys. Rev. Lett.* **1996**, *77*, 3865.
[35] R. F. Zhang, X. D. Wen, D. Legut, Z. H. Fu, S. Veprek, E. Zurek, H. K. Mao, *Sci. Rep.* **2016**, *6*, 23088.
[36] R. F. Zhang, S. Veprek, A. S. Argon, *Phys. Rev. B* **2008**, *77*, 172103.
[37] T. Ma, H. Li, X. Zheng, S. Wang, X. Wang, H. Zhao, S. Han, J. Liu, R. Zhang, P. Zhu, Y. Long, J. Cheng, Y. Ma, Y. Zhao, C. Jin, X. Yu, *Adv. Mater.* **2007**, *29*, 1604003.
[38] A. N. Christensen, *Acta Chem. Scand. A* **1977**, *31*, 77.
[39] G. Brauer, H. Kirner, *Z. Anorg. Allg. Chem.* **1964**, *328*, 34.
[40] W. Utsumi, H. Saitoh, H. Kaneko, T. Watanuki, K. Aoki, O. Shimomura, *Nature Mater.* **2003**, *2*, 735.
[41] F. Birch, *J. Geophys. Res.* **1978**, *83*, 1257.
[42] P. Vinet, J. Ferrante, J. H. Rose, J. R. Smith, *J. Geophys. Res.* **1987**, *92*, 9319.
[43] S. Wang, X. Yu, J. Zhang, M. Chen, J. Zhu, L. Wang, D. He, Z. Lin, R. Zhang, K. Leinenweber, Y. Zhao, *Phys. Rev. B* **2012**, *86*, 064111.
[44] O. Shebanova, E. Soignard, P. F. Mcmillan, *High Press. Res.* **2006**, *26*, 87.
[45] D. Dzivenko, A. Zerr, N. Guignot, M. Mezouar, R. Riedel, *EPL* **2010**, *92*, 66001.
[46] J. O. Kim, J. D. Achenbach, P. B. Mirkarimi, M. Shinn, S. A. Barnett, *J. Appl. Phys.* **1992**, *72*, 1805.
[47] H. Yusa, F. Kawamura, T. Taniguchi, N. Hirao, Y. Ohishi, T. Kikegawa, *J. Appl. Phys.* **2014**, *115*, 103520.
[48] M. T. Yeung, R. Mohammadi, R. B. Kaner, *Annu. Rev. Mater. Res.* **2016**, *46*, 465.
[49] J. B. Levine, S. H. Tolbert, R. B. Kaner, *Adv. Funct. Mater.* **2009**, *19*, 3519.
[50] J. Haines, J. M. Léger, G. Bocquillon, *Annu. Rev. Mater. Res.* **2001**, *31*, 1.
[51] C. M. Zener, S. Siegel, *Elasticity and Anelasticity of Metals*, University of Chicago Press, Chicago **1948**.
[52] X. Yu, R. Zhang, D. Weldon, S. C. Vogel, J. Zhang, D. W. Brown, Y. Wang, H. M. Reiche, S. Wang, S. Du, C. Jin, Y. Zhao, *Sci. Rep.* **2015**, *5*, 12552.
[53] R. F. Zhang, S. H. Sheng, S. Veprek, *Appl. Phys. Lett.* **2009**, *94*, 121903.
[54] R. F. Zhang, D. Legut, R. Niewa, A. S. Argon, S. Veprek, *Phys. Rev. B* **2010**, *82*, 104104.